# LHCb sensitivity to sin($2\beta$) from the CP-asymmetry in $B^0 \to J/\psi(\mu\mu)K^0_S(\pi^+\pi^-)$ decays

**S. Amato[1], M. Calvi[2], M. Gandelman[1], C. Göbel[3], N. Mangiafave[4], S. Poss[5], F. Rodrigues[1]**

[1] Instituto de Física - Universidade Federal do Rio de Janeiro, Brazil
[2] University of Milano-Bicocca and INFN, Milano, Italy
[3] Depto. de Física, Pontifícia Universidade Católica do Rio de Janeiro, Brazil
[4] University of Cambridge, UK
[5] CPPM, Aix-Marseille Université, CNRS/IN2P3, Marseille, France

**Abstract**

This note presents an update of the $B^0 \to J/\psi(\mu\mu)K^0_S(\pi^+\pi^-)$ analysis in order to obtain the LHCb sensitivity to $\sin(2\beta)$. We present two selection criteria, one considering only lifetime unbiased cuts and another which includes lifetime biased cuts to reduce further the background contamination. For an integrated luminosity of 2 fb$^{-1}$ and after L0 trigger, we estimate a yield of 193k events for the $B^0 \to J/\psi(\mu\mu)K^0_S$ channel with the lifetime unbiased selection criteria, with a total background to signal ratio of 3.43. For the lifetime biased selection, the signal yield is 208k events and the background to signal ratio is to 0.63. The statistical sensitivity on $\sin(2\beta)$ is found to be 0.023 and 0.020 for the unbiased and biased selections, respectively.

# 1 Introduction

The decay $B^0 \to J/\psi K^0_S$ is well known as the gold-plated mode for the study of CP violation in the $B^0$-meson system. Here, the $B^0$ meson decays to a CP eigenstate – the final state being common to both $B^0$ and $\overline{B}^0$ – allowing for interference through oscillation. Tree and penguin diagrams for this $B^0$ decay are shown in Fig. 1.

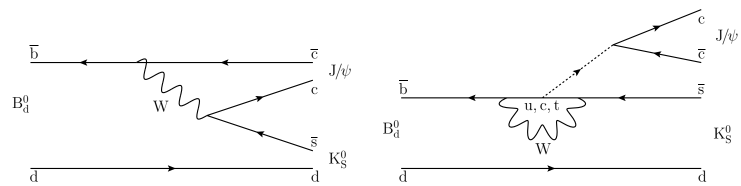


Figure 1: Tree (left) and penguin (right) diagrams for $B^0 \to J/\psi K^0_S$ decay.

Safely neglecting the contribution coming from the penguin topology with internal $u$ quark, we see that no direct CP violation is expected for this decay mode in the Standard Model (SM), $\mathcal{A}^{\rm dir}_{\rm CP} = 0$. Consequently the time-dependent CP asymmetry is due entirely to mixing-induced CP-violation contributions, $\mathcal{A}^{\rm mix}_{\rm CP}$. Considering also that $\Delta\Gamma \approx 0$ for the $B^0$ system, this asymmetry is predicted to be described by a simple expression [1, 2]:

$$\mathcal{A}_{J/\psi K^0_S} \equiv \frac{\Gamma(\overline{B}_d(t) \to J/\psi K^0_S) - \Gamma(B_d(t) \to J/\psi K^0_S)}{\Gamma(\overline{B}_d(t) \to J/\psi K^0_S) + \Gamma(B_d(t) \to J/\psi K^0_S)} = \sin(\Delta m_{B_d} t)\mathcal{A}^{\rm mix}_{\rm CP}, \qquad (1)$$

where $\Delta m_{B_d} = m_{B^0_H} - m_{B^0_L}$ is the mass difference of the two $B^0$ mass eigenstates and $\mathcal{A}^{\rm mix}_{\rm CP} = \sin(2\beta)$ in the SM. This decay mode is also experimentally clean, with relatively low background. Currently, the sensitivity reached by the B-factories are at the level of 4% (see the latest results from Babar [3] and Belle [4]). The current world-averaged result [5] is

$$\sin(2\beta) = 0.673 \pm 0.023 \ . \qquad (2)$$

A mandatory step in extracting $\sin(2\beta)$ is to tag the initial $B^0$ flavour. A careful study of the tagging efficiency, $\varepsilon_{\rm tag}$, and the wrong tag fraction (mistag), $\omega$, is necessary since the measured asymmetry is diluted due to the mistag:

$$\mathcal{A}^{\rm meas}_{J/\psi K^0_S} = (1 - 2\omega)\sin(\Delta m_{B_d} t)\sin(2\beta) \ . \qquad (3)$$

The extraction of $\omega$ is obtained through a control channel – a decay to a self-tagged flavour-specific final state. The natural control channel for $B^0 \to J/\psi K^0_S$ is $B^0 \to J/\psi K^{*0}$, with $K^{*0} \to K^+\pi^-$, where the charge of the kaon indicates the flavour of the $B^0$ at the decay time.

In this note, we present an update of the study of the $B^0 \to J/\psi(\mu\mu)K^0_S$ decay mode aiming to determine the LHCb sensitivity to $\sin(2\beta)$. We describe reconstruction and selection in Section 2. In Section 3 we present event yields and background estimations. In Section 4 we discuss the $B^0$ tagging performance for $B^0 \to J/\psi(\mu\mu)K^0_S$. In Section 5, we present the result for the LHCb sensitivity to $\sin(2\beta)$ for an integrated luminosity of 2 fb$^{-1}$. Finally, summary and conclusions are presented in Section 6.

# 2 Reconstruction and selection

All the sensitivities studies in LHCb are performed by analyzing a large sample of simulated minimum-bias proton-proton interactions at $\sqrt{s} = 14$ TeV, including pile-up, generated using PYTHIA[6]. The generated particles are tracked through the detector material and surrounding environment using GEANT 4 [7] where the geometry and material of the LHCb detector is described, using the Gauss [1] LHCb package. The present study uses the so-called *Data Challenge 2006 (DC06)* data, and the LHCb standard digitization, reconstruction and analysis software, respectively Boole, Brunel and DaVinci [2].

The specific channels are obtained by filtering the minimum bias data-set requiring that the final products of the b-meson lie within the LHCb detector acceptance. The samples used in this analysis are $\mathrm{B^0 \to J/\psi(\mu\mu)K^0_S}$, which is the signal channel used to infer the sensitivity to $\sin(2\beta)$, inclusive $\mathrm{b\overline{b}}$ events (accepted within a 400mrad cone), samples of inclusive $\mathrm{X_b \to J/\psi(\mu\mu)X}$ (with $\mathrm{X_b = B^0, B^+, B^0_s, \Lambda_b}$), events containing a prompt $\mathrm{J/\psi(\mu\mu)}$ as well as minimum bias events to study the background contamination.

For the $\mathrm{J/\psi}$ reconstruction only "long" tracks are used, i.e. tracks that cross the full tracking system, whereas for the $\mathrm{K^0_S}$ selection, due to the long lifetime, "downstream" tracks are also considered. These are tracks which leave hits in the TT and the tracking stations only, i.e. none in the VELO. For details on the LHCb tracking reconstruction and performance see [8].

The particle identification in LHCb is also described in detail in [8]. Basically each detector provides a likelihood for a particle hypothesis and, for each track, the difference in log-likelihood between two hypothesis $a$ and $b$ ($\Delta \ln \mathcal{L}_{\mathrm{ab}}$) is determined.

The selection criteria have been chosen in order to maximize the signal yield keeping the background to a reasonable level. Here we present two sets of selection criteria, according to the use – or not – of cuts that affect the proper time distribution. What we call *lifetime unbiased selection* has higher B/S, but mainly from prompt $\mathrm{J/\psi}$, thus with low proper-time. The *lifetime biased selection* has very low total B/S but needs an acceptance correction, which in general needs to be extracted from simulated events.

## 2.1 $\mathrm{J/\psi \to \mu^+\mu^-}$ Selection

Good candidates for $\mathrm{J/\psi \to \mu^+\mu^-}$ were selected requiring a minimum transverse momentum of both muons, good muon tracks and reconstructed $\mathrm{J/\psi}$ vertex. Besides, a $\mathrm{J/\psi}$ mass window cut is applied; events are required to be within $3\sigma$ of the nominal $\mathrm{J/\psi}$ mass. In Table 1 the selection cuts for $\mathrm{J/\psi \to \mu^+\mu^-}$ are displayed. Further cuts which differ for $\mathrm{B^0 \to J/\psi(\mu\mu)K^0_S}$ lifetime unbiased and biased selection are discussed later.

## 2.2 $\mathrm{K^0_S \to \pi^+\pi^-}$ Selection

The $\mathrm{K^0_S \to \pi^+\pi^-}$ decays are reconstructed according to two categories, depending on the types of tracks: LL category, with two long tracks and DD category, with two downstream tracks to take into account the long lived $\mathrm{K^0_S}$ mesons which are about 2/3 of the selected

[1] Gauss v25r8, http://lhcb-release-area.web.cern.ch/LHCb-release-area/DOC/gauss.
[2] Boole v12r10 (http://lhcb-release-area.web.cern.ch/LHCb-release-area/DOC/boole),
Brunel v31 (http://lhcb-release-area.web.cern.ch/LHCb-release-area/DOC/brunel),
DaVinci v21r0 (http://lhcb-release-area.web.cern.ch/LHCb-release-area/DOC/davinci).

| Variable | | Cut Value |
|---|---|---|
| $p_T(\mu_1,\mu_2)$ [GeV/$c$ ] | $>$ | 0.5 |
| $\chi^2$/ndof $\mu$ tracks | $<$ | 5.0 |
| $\chi^2$/ndof(J/$\psi$) | $<$ | 6.0 |
| $\Delta M$(J/$\psi$) [MeV/$c^2$ ] | $<$ | 41.1 |

Table 1: Cuts applied to select J/$\psi\rightarrow\mu^+\mu^-$ candidates.

sample. Each pair of oppositely-charged pions is fitted to a common vertex. Good $K^0_S$ candidates are selected following the criteria shown in Table 2, which are based on pion quality, $K^0_S$ vertex quality and $K^0_S$ mass window cuts ($3\sigma$ around the nominal mass). Also, given the long life of $K^0_S$, a cut on impact parameter significance IP/$\sigma$ of the pions with respect to the primary vertex (PV) is also applied. At this point, an efficiency of 9.08% is achieved with respect to generated and reconstructed events.

| Variable | | Cut Value - DD | Cut Value - LL |
|---|---|---|---|
| $p(\pi_1,\pi_2)$ [GeV/$c$ ] | $>$ | 2.0 | 2.0 |
| $\chi^2$/ndof $\pi$ tracks | $<$ | 20.0 | 10.0 |
| $\chi^2$/ndof($K^0_S$) | $<$ | 20.0 | 10.0 |
| IP/$\sigma$ ($\pi - PV$) | $>$ | 2.0 | 3.0 |
| $\Delta M$($K^0_S$) [MeV/$c^2$ ] | $<$ | 29.7 | 12.3 |

Table 2: Cuts applied to select $K^0_S\rightarrow\pi^+\pi^-$ candidates.

### 2.3 $B^0\rightarrow$ J/$\psi(\mu\mu)K^0_S$ Selection

In order to select the $B^0\rightarrow$ J/$\psi(\mu\mu)K^0_S$ candidates, the same discriminant variables are used for the two $K^0_S$ categories, but the values of the cuts differ between the two and are shown in Table 3, and discussed below. Two sets of cuts are proposed: the first, using variables that should not introduce any bias to the lifetime distribution and the second, which uses the more effective cuts to reduce the background.

In Table 3, IPCHI2 is the impact parameter $\chi^2$ of the $B^0$ candidate with respect the primary vertex (PV), $\chi^2$/ndof($B$) measures the quality of the $B^0$ vertex, DIRA is the cosine of the angle between momentum of the $B^0$ and the direction of flight from the best PV to the decay vertex, and FDPV is the flight distance of the $B^0$ with respect to the PV. A J/$\psi K^0_S$ mass cut of 60 MeV/$c^2$ around $B^0$ mass is also applied

These selection criteria are the result of an optimization for which the purpose was to achieve a very low minimum bias acceptance rate and also to minimize the $b\overline{b}$ inclusive retention, while keeping a good total signal efficiency.

When running these selections on 5.17M minimum bias L0 stripped events, no event is selected in a $\pm300$ MeV/$c^2$ mass region, corresponding to a rate smaller than 0.42 Hz ( 90% CL) at nominal luminosity ($2\times10^{32}$cm$^{-2}$s$^{-1}$).

| Variable | | Unbiased DD | Unbiased LL | Biased DD | Biased LL |
|---|---|---|---|---|---|
| $DLL(\mu - \pi)$ for $\mu$ | $>$ | -5 | -5 | -5 | -5 |
| $DLL(K - \pi)$ for $\mu$ | $<$ | 2 | 2 | - | - |
| $p_T(\mathrm{J}/\psi)$ [GeV/$c$ ] | $>$ | 1.0 | 1.0 | - | - |
| $p_T(K_S)$ [GeV/$c$ ] | $>$ | 1.0 | 1.0 | - | - |
| IPCHI2 (B-PV) | $<$ | 25.0 | 25.0 | 25.0 | 25.0 |
| $(z_{\mathrm{K^0_S}} - z_{\mathrm{J}/\psi})/\sigma_z$ | $>$ | 0.0 | 0.0 | - | 10.0 |
| $\chi^2/\mathrm{ndof}(B)$ | $<$ | 5.0 | 15.0 | 10.0 | 15.0 |
| $\chi^2/\mathrm{ndof}(K_S)$ | $<$ | - | - | 10.0 | 10.0 |
| DIRA | $>$ | - | - | 0.9996 | 0.9996 |
| FDPV (J/$\psi$) | $>$ | - | - | - | 0.25 |
| $\Delta M(\mathrm{J}/\psi \mathrm{K^0_S})$ [MeV/$c^2$] | $<$ | 60 | 60 | 60 | 60 |

Table 3: Cuts applied to select $\mathrm{B^0} \to \mathrm{J}/\psi(\mu\mu)\mathrm{K^0_S}$ candidates for the two $\mathrm{K^0_S}$ categories.

| Selection | sel. LL | sel. DD | sel. TOTAL |
|---|---|---|---|
| Unbiased | 23629 | 62219 | 85848 |
| Biased | 29124 | 63807 | 92931 |

Table 4: Number of L0 triggered and selected events of $\mathrm{B^0} \to \mathrm{J}/\psi(\mu\mu)\mathrm{K^0_S}$ for the lifetime unbiased and biased selections, from a total of 1316142 generated events within the geometrical acceptance.

## 2.4 $\mathrm{B^0} \to \mathrm{J}/\psi(\mu\mu)\mathrm{K^0_S}$ Selected Sample

In Table 4 we show, for both lifetime unbiased and biased selections, the number of selected events for LL and DD $\mathrm{K^0_S}$ categories separetely and the number of total selected events, all after L0 trigger, which has an efficiency of 94%. The total efficiency is $\varepsilon_{\mathrm{tot}} = \varepsilon_{\mathrm{geom}} \times \varepsilon_{\mathrm{sel/gen}}$ where sel is the number of selected events (including L0 trigger), gen is the corresponding number of generated events (gen = 1316142) and $\varepsilon_{\mathrm{geom}}$ is the geometric acceptance of the event generation. These efficiencies are displayed in Table 5.

The $\mathrm{B^0}$ mass distribution is fitted to a double Gaussian, as shown in Figure 2. It has core and tail resolutions of 13.6 MeV/$c^2$ and 22.2 MeV/$c^2$, respectively, with 54% of the events falling into the core. A 2 MeV/$c^2$ bias in the $\mathrm{B^0}$ mass with respect to the generated value (5279 MeV) is due to photon production not taken into account in the reconstruction. The proper time distribution is shown in Figure 3. The result of a simple

| Selection | $\varepsilon_{\mathrm{sel/gen}}$ | $\varepsilon_{\mathrm{geom}}$ | $\varepsilon_{\mathrm{tot}}$ |
|---|---|---|---|
| Unbiased | $(6.52 \pm 0.03) \times 10^{-2}$ | $0.207 \pm 0.004$ | $(1.35 \pm 0.03) \times 10^{-2}$ |
| Biased | $(7.06 \pm 0.02) \times 10^{-2}$ | $0.207 \pm 0.004$ | $(1.46 \pm 0.03) \times 10^{-2}$ |

Table 5: Efficiencies for signal for lifetime unbiased and biased selections after L0 trigger requirements.

exponential fit gives $\tau_B = 1.526 \pm 0.005$ ps. Fitting separetely for DD and LL $\mathrm{K_S^0}$ types, the values change to $\tau_B(\mathrm{DD}) = 1.536 \pm 0.007$ ps and $\tau_B(\mathrm{LL}) = 1.48 \pm 0.01$ ps. For the unbiased selection we find no appreciable dependence of the proper time distribution on the cuts. The proper time resolution is given in Figure 4; it has core and tail resolutions of 35 ps and 77 ps, respectively, with 75% of the events falling into the core.

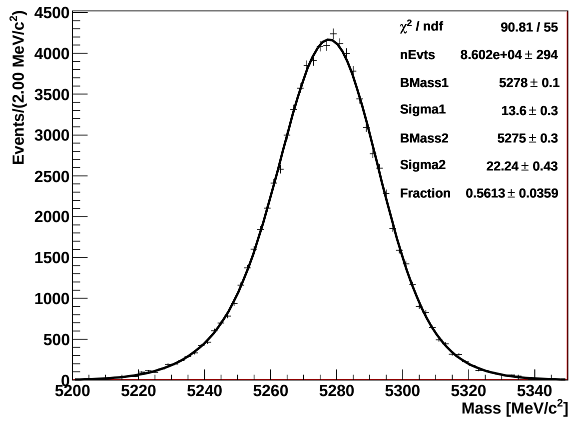


Figure 2: Invariant mass distribution for $\mathrm{B^0} \to \mathrm{J}/\psi(\mu\mu)\mathrm{K_S^0}$ after the lifetime unbiased selection cuts.

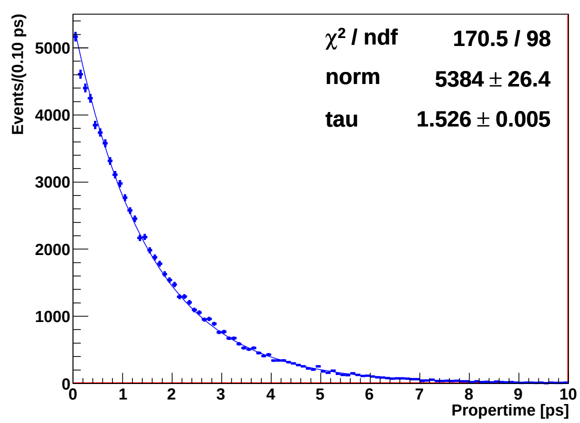


Figure 3: Proper time distribution for signal events, for the lifetime unbiased selection.

For the lifetime biased selection, we have to take into account the proper time acceptance function, obtained by the ratio between the proper time distribution after full selection and the one we obtain after reconstruction, with very loose cuts which presents no lifetime bias effect. In Figure 5 we show this distribution. It is fitted to the empirical function

$$\mathrm{acc}(t) = b(1 - e^{at}), \tag{4}$$

where $b$ reflects an arbitrary scale and $a$ gives the slope of the acceptance function and it is found to be $a = -5.94 \pm 0.07\ \mathrm{ps}^{-1}$.

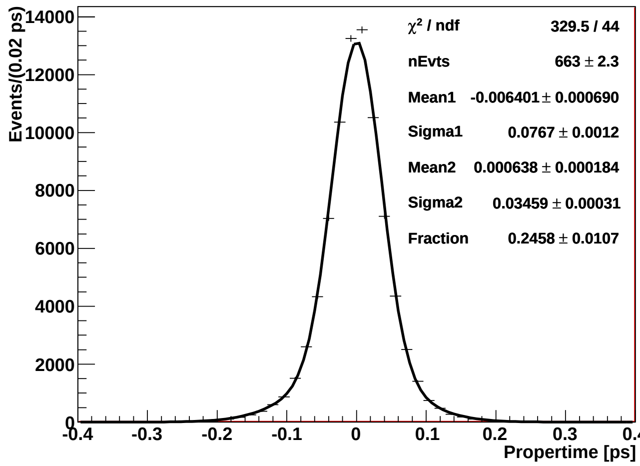


Figure 4: Proper time resolution of signal events, for the lifetime unbiased selection.

| Sample | Selection | sel. LL | sel. DD | sel. TOTAL |
|---|---|---|---|---|
| inclusive $b\overline{b}$ | Unbiased | 6 | 18 | 24 |
| | Biased | 9 | 12 | 21 |

Table 6: Number of L0 triggered and selected events of inclusive $b\overline{b}$ for the lifetime unbiased and biased selections, from the 25.23M generated events within the geometrical acceptance.

## 2.5 $b\overline{b}$ inclusive sample

One of the background sources analysed is a set of 25.23M events of inclusive $b\overline{b}$ sample.

To increase the statistical power of this sample, a 300 MeV/$c^2$ window around the nominal $B^0$ mass is used to estimate the background. Assuming that this combinatoric background follows a uniform distribution throughout this wider window we can estimate the number of events in the narrower 60 MeV/$c^2$ window.

Even with this procedure, the number of events is very low after the final $B^0$ cuts, as we shall see later, so for the purpose of extracting the lifetime parameter out of this sample, we applied only the $J/\psi$ and $K^0_S$ selection criteria. Since the prompt $J/\psi$ will be considered separately, we have discarded from this sample the events where the $J/\psi$ comes from the primary vertex.

The proper time distribution of this sample is shown in Fig. 6 and a double exponential is fitted to it. The fit parameters obtained are $\tau_1 = 1.50 \pm 0.12$ ps and $\tau_2 = 0.07 \pm 0.02$ ps for the long and short lifetime respectively, with 80% of the events falling into the long lifetime component. The large peak at very short lifetime was investigated and found to be mainly due to ghosts (particles with no MC true particle associated to it) and the rest are events where one of the final state particles come from the primary vertex.

The mass distribution is shown in Fig. 7, also fitted to an exponential.

After the full $B^0 \to J/\psi(\mu\mu)K^0_S$ selection criteria described previously, we obtain the results shown in Table 6.

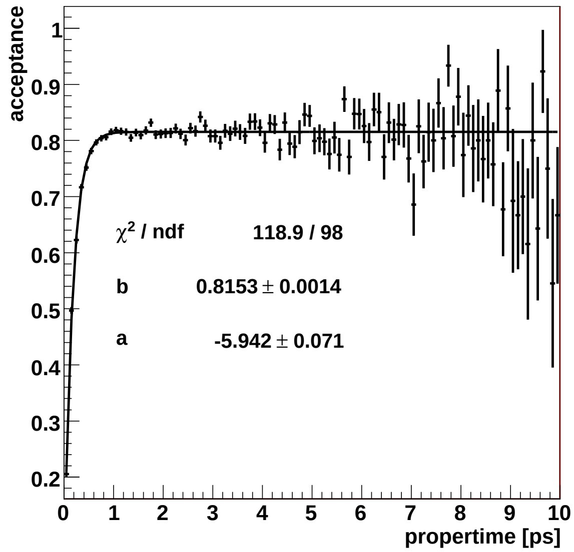


Figure 5: Proper time acceptance distribution for lifetime biased selection.

| Sample | Selection | $\varepsilon_{\rm sel/gen}$ | $\varepsilon_{\rm geom}$ | $\varepsilon_{\rm tot}$ |
|---|---|---|---|---|
| inclusive $\rm b\overline{b}$ | Unbiased | $(9.5 \pm 1.9) \times 10^{-7}$ | $0.437 \pm 0.001$ | $(4.16 \pm 0.85) \times 10^{-7}$ |
| | Biased | $(8.3 \pm 1.8) \times 10^{-7}$ | $0.437 \pm 0.001$ | $(3.64 \pm 0.79) \times 10^{-7}$ |

Table 7: Efficiencies for inclusive $\rm b\overline{b}$ for lifetime unbiased and biased selections, evaluated in a 300 MeV/$c^2$ window, after L0 trigger requirements.

A closer look at the 24 events that survive the unbiased and the biased selections is presented in Appendix A.

To obtain the total efficiency, shown in Table 7, again we use $\varepsilon_{\rm tot} = \varepsilon_{\rm geom} \times \varepsilon_{\rm sel/gen}$.

#### 2.5.1 $X_{\rm b} \to J/\psi{\rm X}$ samples

To cross check the inclusive $\rm b\overline{b}$ yield, we performed the analysis on some $X_{\rm b} \to J/\psi{\rm X}$ available samples, which are listed in Table 8, together with the number of generated and surviving events after each selection. The total efficiency is computed using $\varepsilon_{\rm geom} = 0.2048$ and their values for each sample is shown in the last column of the same table. It should be mentioned that the true $\rm B^0 \to J/\psi(\mu\mu)K^0_S$ events are removed from the $\rm B_d \to J/\psi X$ sample.

Since we have more events surviving the final $\rm B_d$ selection in the four samples than in the inclusive $\rm b\overline{b}$, we take the background shape of the proper time distribution of their combination, which has been obtained by summing each normalized histogram weighted by the expected final yields, as described later in Sect. 3 (see Table 11). For the lifetime unbiased selection, a double exponential is fitted to the proper time, with the parameters being $\tau_1 = 0.35 \pm 0.04$ ps and $\tau_2 = 1.6 \pm 0.2$ ps for the short and long lifetime respectively with 70% of the events in the short one. The plot is shown in Figure 8(a). For the

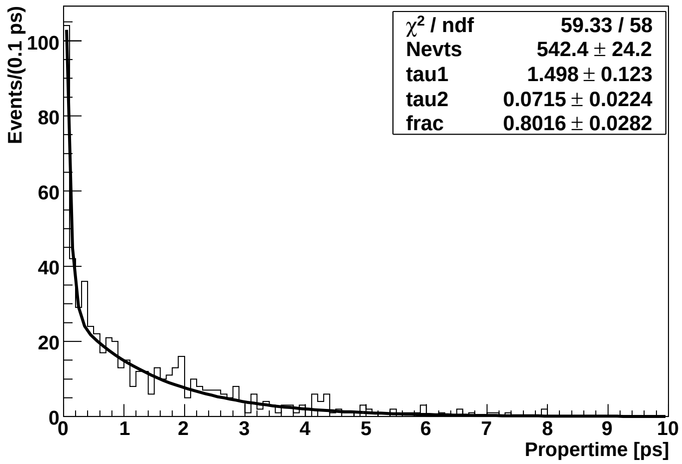


Figure 6: Proper time distribution for $b\overline{b}$ inclusive, after $J/\psi$ and $K^0_S$ selection criteria.

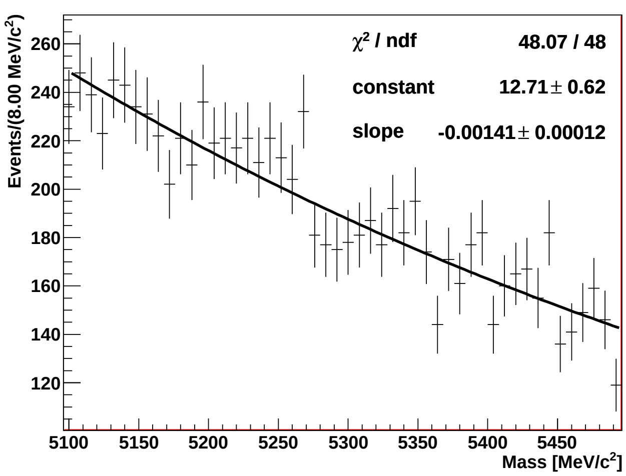


Figure 7: Mass distribution for $b\overline{b}$ inclusive, after $J/\psi$ and $K^0_S$ selection criteria.

| Sample | Generated | Selection | sel. LL | sel. DD | sel. TOTAL | $\varepsilon_{\rm tot}$ |
|---|---|---|---|---|---|---|
| $B_u \to J/\psi X$ | 3261566 | Unbiased | 114 | 329 | 443 | $(2.78 \pm 0.13) \times 10^{-5}$ |
| | | Biased | 272 | 512 | 784 | $(4.92 \pm 0.18) \times 10^{-5}$ |
| $B_d \to J/\psi X$ | 2830411 | Unbiased | 196 | 555 | 751 | $(5.43 \pm 0.20 \times 10^{-5}$ |
| | | Biased | 390 | 636 | 1026 | $(7.42 \pm 0.23) \times 10^{-5}$ |
| $B_s \to J/\psi X$ | 490767 | Unbiased | 19 | 65 | 84 | $(3.51 \pm 0.38) \times 10^{-5}$ |
| | | Biased | 48 | 87 | 135 | $(5.63 \pm 0.48) \times 10^{-5}$ |
| $\Lambda_b \to J/\psi X$ | 80012 | Unbiased | 15 | 95 | 110 | $(2.82 \pm 0.27) \times 10^{-4}$ |
| | | Biased | 25 | 95 | 120 | $(3.07 \pm 0.28) \times 10^{-4}$ |

Table 8: Number of generated and selected events of $X_b \to J/\psi X$ for the lifetime unbiased and biased selections, after L0 trigger requirements.

lifetime biased selection, a good description of the distribution is obtaining by fitting it to a double exponential (with free parameters) times the acceptance function obtained for signal events (Eq. 4), with parameter $a$ fixed[3]. The fitted distribution and fit parameters are shown in Figure 8(b).

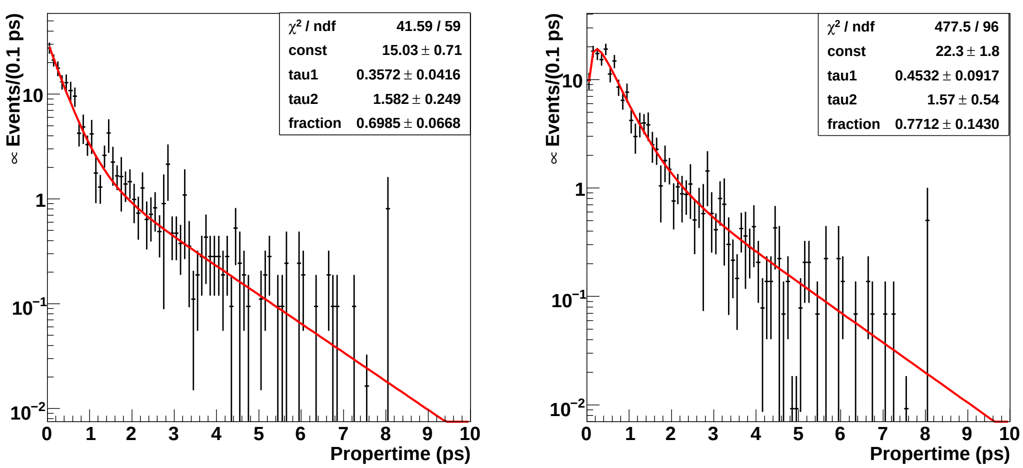


(a) (b)

Figure 8: Proper time distribution for the combination of $B_u \to J/\psi X$, $B_d \to J/\psi X$, $B_s \to J/\psi X$ and $\Lambda_b \to J/\psi X$ samples after the full $B_d$ selection. (a) Lifetime unbiased selection (b) Lifetime biased selection.

### 2.6 Prompt $J/\psi$ samples

An important source of background for the lifetime unbiased selection are events where the $J/\psi$ comes from the primary vertex, the prompt $J/\psi$. This set of events is obtained from the inclusive $J/\psi$ sample by excluding true $X_b \to J/\psi X$ events during analysis. To

[3]The fit does not improve by letting $a$ free: it returns a compatible value with a high error.

| Sample | Selection | sel. LL | sel. DD | sel. TOTAL |
|---|---|---|---|---|
| prompt $J/\psi$ | Unbiased | 467 | 1188 | 1655 |
| | Biased | 41 | 119 | 160 |

Table 9: Number of L0 triggered and selected events of prompt $J/\psi$ for the lifetime unbiased and biased selections, from the 2.50M generated events within the geometrical acceptance.

| Sample | Selection | $\varepsilon_{\mathrm{sel/gen}}$ | $\varepsilon_{\mathrm{geom}}$ | $\varepsilon_{\mathrm{tot}}$ |
|---|---|---|---|---|
| prompt $J/\psi$ | Unbiased | $(6.62 \pm 0.16) \times 10^{-4}$ | 0.197 | $(1.30 \pm 0.03) \times 10^{-4}$ |
| | Biased | $(6.40 \pm 0.51) \times 10^{-5}$ | 0.197 | $(1.26 \pm 0.10) \times 10^{-5}$ |

Table 10: Efficiencies for prompt $J/\psi$ for lifetime unbiased and biased selections, evaluated in a 300 MeV/$c^2$ window, after L0 trigger requirements.

reduce the statistical uncertainty on the number of selected events, the same procedure of considering events in an enlarged mass window of $\pm 300$ MeV/$c^2$ is used for selection on these samples.

Applying the selection criteria on 2498579 generated inclusive $J/\psi$ events, we obtain the results shown in Table 9. The efficiencies calculated as described in the $b\overline{b}$ section, are shown in Table 10.

The prompt $J/\psi$ proper time for the unbiased and biased selections are shown in Figs. 9. Since the $J/\psi$ decays promptly, its proper time distribution comes from time resolution only; for the lifetime unbiased selection it is fitted to a double Gaussian; for the lifetime biased selection it is fitted empirically to a double Gaussian (with common mean fixed to zero) times a Landau function. The mass distribution prompt $J/\psi$ events after the lifetime unbiased selection is shown in Fig. 10 and fitted to a single exponential.

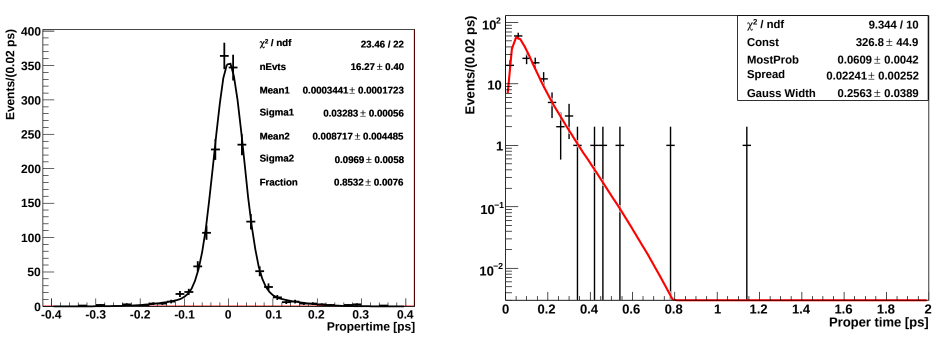


(a) (b)

Figure 9: Proper time distribution for prompt $J/\psi$ for the lifetime unbiased (a) and biased (b) selections.

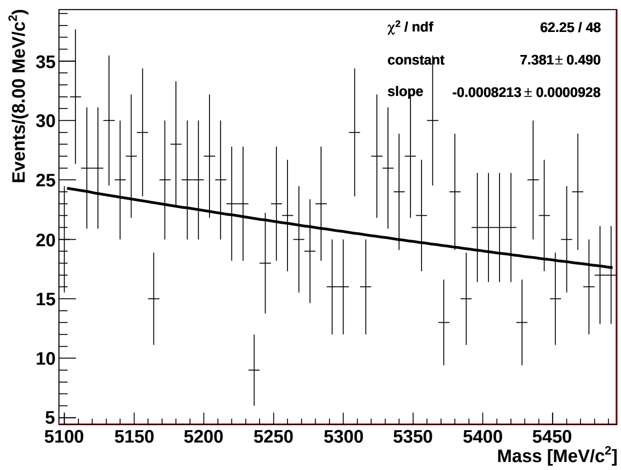


Figure 10: Mass distribution for prompt J/$\psi$ in the unbiased selection.

# 3 Event yield and background estimation

The annual signal event yield is computed as

$$S = \mathcal{L}_{\text{int}} \times \sigma_{b\overline{b}} \times 2 \times f_{\text{B}} \times \text{BR}_{\text{vis}} \times \varepsilon_{\text{tot}}, \tag{5}$$

for a nominal annual integrated luminosity of $\mathcal{L}_{\text{int}} = 2$ fb$^{-1}$ ($10^7$ s at $2 \times 10^{32}$ cm$^{-2}$s$^{-1}$) and a b$\overline{\text{b}}$ production cross section of $\sigma_{b\overline{b}} = 500$ $\mu$b. The probability for a b-quark to hadronize into a hadron is assumed to be $f_{\text{B}} = 0.405$ for $\text{B}^0$ and the factor 2 takes into account the production of both b- and $\overline{\text{b}}$-hadrons. The visible branching ratio $\text{BR}_{\text{vis}}$ is the product of all branching ratios involved in the b-hadron of interest. In the case of $\text{B}^0 \to \text{J}/\psi(\mu\mu)\text{K}^0_{\text{S}}$, the visible branching ratio $\text{BR}_{\text{vis}}$ is $(1.787 \pm 0.068) \times 10^{-5}$ [10].

The total efficiency obtained for signal events, according to the previous section, is $1.35 \pm 0.03$ % for the lifetime unbiased selection and $1.46 \pm 0.03$ % for the lifetime biased selection. The estimated annual yields, calculated after L0 trigger, are 193k and 208k for the lifetime unbiased and biased selections respectively.

In order to estimate the B/S ratio, calculated after L0 trigger, two samples have been used, the inclusive b$\overline{\text{b}}$ and prompt $\text{J}/\psi \to \mu^+\mu^-$, described in the previous section. The yields for these two sources are obtained from the total efficiencies shown in Tables 7 and 10 . For b$\overline{\text{b}}$ the yield for 2fb$^{-1}$ is given by:

$$B_{b\overline{b}} = \mathcal{L}_{\text{int}} \times \sigma_{b\overline{b}} \times \text{window factor} \times \varepsilon_{\text{tot}} \tag{6}$$

where window factor = 0.2 is to rescale the mass window to 60 MeV/$c^2$ and $\sigma_{b\overline{b}} = 500\mu b$. The yield after L0 trigger is then 82K for the unbiased selection and 72K for the biased selection. This results in a B/S of $0.42 \pm 0.09$ and $0.36 \pm 0.08$ for the unbiased and biased selection, respectively. If we consider only the events that falls into the inclusive b$\overline{\text{b}}$ background category (13 for the unbiased and 11 for the biased), the B/S turns into 0.23$\pm$ 0.06 and 0.18$\pm$0.05.

This result can be compared with the B/S obtained from the dedicated $X_{\text{b}} \to J/\psi$X samples. The yield is obtained with the same expression for the signal (equation 5) where

| Sample | $BR_{vis}$ | Selection | B/S |
|---|---|---|---|
| $B_u \to J/\psi X$ | $6.29\times10^{-5}$ | Unbiased | $(7.25 \pm 0.37) \times 10^{-3}$ |
| | | Biased | $(11.86 \pm 0.48) \times 10^{-3}$ |
| $B_d \to J/\psi X$ | $3.14\times10^{-4}$ | Unbiased | $(70.7 \pm 2.9) \times 10^{-3}$ |
| | | Biased | $(89.2 \pm 3.3) \times 10^{-3}$ |
| $B_s \to J/\psi X$ | $4.67\times10^{-4}$ | Unbiased | $(67.8 \pm 7.5) \times 10^{-3}$ |
| | | Biased | $(100.7 \pm 8.9) \times 10^{-3}$ |
| $\Lambda_b \to J/\psi X$ | $2.30\times10^{-5}$ | Unbiased | $(26.8 \pm 2.6) \times 10^{-3}$ |
| | | Biased | $(27.0 \pm 2.5) \times 10^{-3}$ |
| $X_b \to J/\psi X$ | | Unbiased | $0.172 \pm 0.008$ |
| Total | | Biased | $0.229 \pm 0.010$ |

Table 11: B/S ratio for each $X_b \to J/\psi X$ samples.

| | Unbiased Selection | | | | Biased Selection | | | |
|---|---|---|---|---|---|---|---|---|
| Sample | Tagg. Eff. | HLT1 | HLT2 | Yield | Tagg. Eff. | HLT1 | HLT2 | Yield |
| Signal | 52% | 78.2% | 95% | 75k | 52% | 90.8% | 95% | 94k |
| Inclusive $b\bar{b}$ | 67% | 78.2% | 95% | 41k | 67% | 90.8% | 95% | 41k |
| Prompt $J/\psi$ | 26% | 78.2% | 95% | 112k | 25% | 90.8% | 95% | 12k |

Table 12: Tagging efficiencies, HLT efficiencies and final yields for 2 $fb^{-1}$. The HLT efficiencies for the background are taken as being the same as for the signal.

$BR_{vis}$ for each channel is given in Table 11 and the efficiencies are taken from Table 8. Combining the B/S from each one of these channels (also shown in Table 11), we obtain a B/S of 0.172 for the unbiased selection and 0.229 for the biased one, compatible with the result from the inclusive $b\bar{b}$ sample.

For prompt $J/\psi$, the yield is obtained by

$$B_{J/\psi\,\mathrm{prompt}} = \mathcal{L}_{\mathrm{int}} \times \sigma_{J/\psi} \times BR_{vis} \times \text{window factor} \times \varepsilon_{tot} \tag{7}$$

where $\sigma_{J/\psi} = 266\ \mu b$, $BR_{vis} = 0.0593$ and the window factor $= 0.2$. The B/S for prompt $J/\psi$, after L0 trigger, is then $3.01 \pm 0.38$ and $0.27 \pm 0.11$ for the unbiased and biased selection, respectively.

For the $\sin(2\beta)$ sensitivity estimate, the high level trigger (HLT) and tagging efficiencies as well as the mistag rate should be taken into account. The tagging performance is discussed in the next section. The high level trigger is divided in two levels and the efficiencies are presented separately for HLT1 and HLT2. For the unbiased lifetime selection, only the unbiased di–muon HLT1 is considered in order to keep avoiding any lifetime bias effect, while for the biased selection the global HLT1 can be used. We show tagging efficiencies together with yields after HLT and tagging in Table 12 for both unbiased and biased selections. It should be emphasized that the details and indeed overall strategy for the HLT are still under development, and hence the performance is expected to evolve with time.

# 4 Tagging

The flavour tagging algorithms described in [11] have been used in this analysis. The tagging efficiencies are directly measured on the signal and background event samples and the same procedure will also be used when analysing real data.

The mistag rate for the signal $B^0 \to J/\psi(\mu\mu)K^0_S$ events can not be measured directly on data, but must be taken from measurements performed on other channels, with flavour specific final states. Tagging performance, however, is not completely independent of the signal channel since trigger and event selection can affect the opposite b hadron kinematic distributions (see [11] for a full discussion). As a consequence, the most suited control channels for $B^0 \to J/\psi(\mu\mu)K^0_S$ are the $B^+ \to J/\psi(\mu\mu)K^+$ and $B^0 \to J/\psi(\mu\mu)K^{*0}$ channels. Having all a $J/\psi(\mu\mu)$ particle, they will be triggered in the same way, using the di-muon lines, and they can also share the same selection criteria, for what concerns the $J/\psi(\mu\mu)$ part. As a result, we expect similar tagging performances on the three channels. This is shown in Table 13 for the $B^0 \to J/\psi(\mu\mu)K^0_S$ and the $B^0 \to J/\psi(\mu\mu)K^{*0}$ channels (we refer to [12] for a similar table for $B^+ \to J/\psi(\mu\mu)K^+$ events and for additional details on the table contents.) The unbiased-lifetime selection described in [13] has been used for the control channels. The mistag values in these tables are calculated by comparing the tagging results with the b-flavour determined from Monte Carlo truth. Events are required to pass the L0 trigger and only reconstructed signal events with tracks matching to the generated Monte Carlo ones are used. The first part of the tables contains the performance of each tagger alone. The second part of the tables show the combined performances which are obtained by sorting all events into five exclusive samples of increasing tagging purity and summing over these samples. The average performance reported in the tables are calculated on all events, not sorted into samples.

The mode $B^+ \to J/\psi(\mu\mu)K^+$ will be mainly used to calibrate in data the flavour tagging performance, while we plan to use the $B^0 \to J/\psi(\mu\mu)K^{*0}$ channel to measure the mistag rate in data from a fit to flavour oscillation as a function of proper time. The full procedure is described in detail in [12]. The numbers in the tables show that there is indeed a good general agreement in the tagging performance among control channels and CP channel, when one consider the contribution of the opposite side (OS) taggers. A small difference between the signal and the control channel appears in the value of the mistag rate for the opposite side pion tag. This is related to the dependence of the same side pion tag mistag on the B transverse momentum (see [12]), and to the softer $p_T$ spectrum for selected $B^0 \to J/\psi K^0_S$ events. A correction can be introduced in the future to take this effect into account.

The true value of the combined mistag rate $\omega = 0.359$ will be used in the following toy studies performed to estimate the sensitivity to $\sin 2\beta$. The use of a combined mistag value and a fit to a single sample instead of a simultaneous fit to the 5 tagging categories (defined in [12]) show identical results.

# 5 Sensitivity to sin(2$\beta$)

## 5.1 sin 2$\beta$ from DC06 signal events

The full Monte Carlo (DC06) used for this analysis has been generated with CP Violation effects included, according to the expected Standard Model asymmetry in Eq. 1. A value

| $B^0 \to J/\psi(\mu\mu)K^0_S$ | | | |
|---|---|---|---|
| | $\varepsilon_{tag}(1-2\omega)^2$ % | $\varepsilon_{tag}$ % | $\omega$ % |
| $\mu$ | 0.74±0.08 | 5.74±0.12 | 32.1±1.0 |
| e | 0.40±0.06 | 2.72±0.08 | 30.9±1.4 |
| $K_{opp}$ | 1.80±0.13 | 14.64±0.18 | 32.5±0.6 |
| $\pi_{same}$ | 0.66±0.08 | 18.09±0.20 | 40.5±0.6 |
| $Q_{vtx}$ | 1.03±0.10 | 42.61±0.25 | 42.2±0.4 |
| Average all taggers | 2.93±0.17 | 52.91±0.26 | 38.24±0.34 |
| **Combined all taggers** | **4.20±0.19** | **52.91±0.26** | **35.92±0.34** |
| Average OS only | 2.35±0.16 | 44.28±0.25 | 38.47±0.37 |
| Combined OS only | 3.45±0.17 | 44.28±0.25 | 36.04±0.37 |
| $B^0 \to J/\psi(\mu\mu)K^{*0}$ | | | |
| | $\varepsilon_{tag}(1-2\omega)^2$ % | $\varepsilon_{tag}$ % | $\omega$ % |
| $\mu$ | 0.78±0.05 | 5.54±0.07 | 31.2±0.6 |
| e | 0.39±0.03 | 2.69±0.05 | 30.9±0.8 |
| $K_{opp}$ | 1.63±0.07 | 14.11±0.10 | 33.0±0.4 |
| $\pi_{same}$ | 1.16±0.06 | 20.35±0.12 | 38.1±0.3 |
| $Q_{vtx}$ | 1.07±0.06 | 42.73±0.14 | 42.1±0.2 |
| Average all taggers | 3.25±0.10 | 53.60±0.15 | 37.69±0.19 |
| **Combined all taggers** | **4.52±0.11** | **53.60±0.15** | **35.48±0.19** |
| Average OS only | 2.28±0.09 | 43.59±0.14 | 38.62±0.21 |
| Combined OS only | 3.45±0.10 | 43.95±0.14 | 36.00±0.21 |

Table 13: Flavour tagging performance for $B^0 \to J/\psi K^0_S$ events (upper) and $B^0 \to J/\psi K^{*0}$ events (lower), after lifetime-unbiased selections and Level-0 trigger requirements. Effective tagging efficiency, tagging efficiency and mistag rate are shown for individual taggers and for their combination. The mistag rate is calculated using the MC truth information. Average: result from the global tagging decision for all events together. Combined: results after splitting into 5 tagging categories. In the last two lines of the tables opposite side (OS) taggers only are used. Uncertainties are statistical.

of $\sin 2\beta = 0.7$ was assigned. As a cross check, $\sin 2\beta$ was measured in our Monte Carlo sample, using only signal events, passing the lifetime unbiased selection. The sample of data corresponds to a statistic of about 0.88 $fb^{-1}$. The fit was performed both using the average value of the mistag and by fitting according to the five tagging categories, as in Table 13. The fit with the average (true) mistag value of $\omega = 0.381$ returned $\sin 2\beta = 0.641 \pm 0.033$. The CP asymmetry as a function of proper time and the corresponding fit are shown in Fig. 11. The combined fit of the five samples according to the tagging categories returned $\sin 2\beta = 0.636 \pm 0.028$.

## 5.2 Sensitivity of $\sin 2\beta$ for 2$fb^{-1}$ from Toy MC studies

To assess the statistical sensitivity of $\sin(2\beta)$ from $B^0 \to J/\psi K^0_S$ corresponding to 2 $fb^{-1}$, a toy Monte Carlo study is performed using the RooFit toolkit [14] by including yields and models for signal and backgrounds as obtained from fully simulated and reconstructed

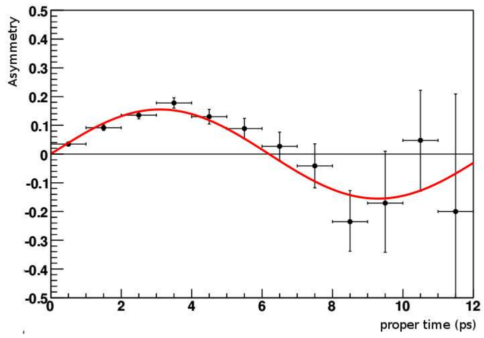


Figure 11: Measured CP asymmetry as a function of proper time for Monte Carlo (DC06) signal events, corresponding to an integrated luminosity of about 0.88 $\mathrm{fb}^{-1}$.

events, described in the previous sections. We present results for models based on both lifetime unbiased and biased selection criteria.

The complete PDF is a sum of the combined mass and proper time PDF's for signal, long lifetime (bb-inclusive) and prompt $J/\psi$ components.

The signal mass is described by a double Gaussian function, according to the fitted distribution found in Fig.2. For simplicity, we use here a common mean ($m_B = 5277\,\mathrm{MeV}/c^2$). The signal proper time PDF is given by

$$\Gamma(t) \propto \mathrm{e}^{-t/\tau_{\mathrm{sig}}} \left[1 + q(1 - 2\omega_{\mathrm{sig}}) \sin 2\beta \sin(\Delta m_{B_d} t)\right] \ . \tag{8}$$

In the expression above, $q$ is the flavour of the $\mathrm{B}^0$, determined from the tagging algorithm, and is $q = 1$ ($q = -1$) for $\mathrm{B}^0$ ($\overline{\mathrm{B}}^0$) events, $\omega_{\mathrm{sig}}$ is the mistag fraction, $\Delta m_{B_d} = 0.507\ \mathrm{ps}^{-1}$, and $\tau_{\mathrm{sig}}$ is the $\mathrm{B}^0$ proper time. For the lifetime biased selection the above function is multiplied by the acceptance function (Eq. 4, Fig. 5).

The total background PDF is the sum of a prompt and a non prompt (LLived) components. The mass distribution is described in both cases by an exponential (see Figs. 7 and 10). For the lifetime unbiased model, the proper time distribution is a double Gaussian for the prompt (Fig. 9(a)) and a double exponential (Fig. 8(a)) for the LLived one. The proper time resolution model for both signal and LLived components is the same double Gaussian as for the prompt component, since it is from the latter that the resolution can be extracted directly. This is also well justified by noticing that the signal and prompt $J/\psi$ proper time resolutions are very similar (see Figs. 4 and 9(a)). Furthermore, we have checked that if we use for generation the corresponding signal and prompt proper time double Gaussian parameters but fit with a common double Gaussian, the difference in all other fitting parameters are negligible.

For the lifetime biased model, the proper time functions obtained by the fitted distributions shown in Fig. 8(b) (long lifetime background) and Fig. 9(b) are used for the LLived and prompt components, respectively, and the proper time resolution model is a double Gaussian with fixed parameters.

For generation of the toy samples, we assume 2 $\mathrm{fb}^{-1}$ yields after full trigger and tagging, as presented in Table 12. The mass range used for generation was $\pm 150\ \mathrm{MeV}/c^2$ around the $\mathrm{B}^0$ mass thus yields for backgrounds were rescaled by a factor of 2.5. An extended unbinned maximum Likelihood fit formalism is used.

For the lifetime unbiased model, an example of a single generation and fit result is presented in Table 14. Generated and fitted PDF distributions for mass and time are shown respectively in Figs. 12 and 13. The resulting asymmetry distribution and fit is shown in Fig. 14. The error on $\sin 2\beta$ is found to be 0.023. This result is confirmed by a full study with 809 toy samples, as shown in Fig. 15.

| **Fixed parameters** | | | |
|---|---|---|---|
| **Parameter** | **Initial value** | | |
| $\Delta m_{\rm d}$ ( $\rm ps^{-1}$ ) | 0.507 | | |
| $\omega_{\rm tag}$ | 0.359 | | |
| **Free parameters** | | | |
| **Parameter** | **Initial value** | **Fitted value** | **Glob. corr.** |
| N events signal | 75881 | $75884 \pm 386$ | 0.56 |
| N events Prompt | $1.1305 \times 10^5$ | $1.1310 \times 10^5 \pm 273$ | 0.57 |
| N events LLived 1 | 12166 | $12070 \pm 289$ | 0.92 |
| N events LLived 2 | 28386 | $28206 \pm 278$ | 0.83 |
| $M_{\rm B}$ ( MeV/$c^2$) | 5277.0 | 5277.0 $\pm 0.1$ | 0.13 |
| $\sigma^{\rm sig}_{\rm mass1}$ ( MeV/$c^2$) | 14 | $14.9 \pm 0.4$ | 0.97 |
| $\sigma^{\rm sig}_{\rm mass2}$ ( MeV/$c^2$) | 22 | $25.0 \pm 1.6$ | 0.98 |
| $\rm frac^{sig}_{mass1}$ | 0.57 | 0.52 $\pm 0.10$ | 0.99 |
| mass slope Prompt ( MeV/$c^2)^{-1}$ | $-1.0 \cdot 10^{-3}$ | $(-0.98 \pm 0.02) \cdot 10^{-3}$ | 0.44 |
| mass slope LLived 1( MeV/$c^2)^{-1}$ | $-1.4 \cdot 10^{-3}$ | $(-1.35 \pm 0.11) \cdot 10^{-3}$ | 0.68 |
| mass slope LLived 2( MeV/$c^2)^{-1}$ | $-1.4 \cdot 10^{-3}$ | $(-1.34 \pm 0.07) \cdot 10^{-3}$ | 0.62 |
| background $\tau^{\rm LL1}$ (ps) | 1.581 | $1.576 \pm 0.022$ | 0.81 |
| background $\tau^{\rm LL2}$ (ps) | 0.357 | $0.353 \pm 0.004$ | 0.81 |
| time resol. $\sigma_{t1}$ (ps) | 0.037 | $0.0368 \pm 0.0002$ | 0.84 |
| time resol. $\sigma_{t2}$ (ps) | 0.090 | $0.0885 \pm 0.0011$ | 0.89 |
| $\rm frac^{Pr}_{time}$ | 0.80 | $0.794 \pm 0.005$ | 0.89 |
| $\tau^{\rm sig}$ (ps) | 1.536 | $1.533 \pm 0.007$ | 0.33 |
| $\sin 2\beta$ | 0.700 | $0.694 \pm 0.023$ | 0.06 |

Table 14: Input parameters for the $\sin 2\beta$ fit and results of a single toy, according to the unbiased model.

For the biased selection, the results for a single toy are displayed in Table 15. Generated and fitted PDF distributions for mass and time are shown respectively in Figs. 16 and the resulting asymmetry distribution and fit is shown in Fig. 17. From a study with 600 toy samples, the error on $\sin 2\beta$ is found to be 0.020 for the lifetime biased selection, see Fig. 18.

We observe that the two selections return significantly different sensitivities on $\sin 2\beta$, with the 2 $\rm fb^{-1}$ statistical uncertainty being 0.023 and 0.020 for the lifetime unbiased and biased respectively. This difference is mainly due to the expected number of signal events of the two selections.

A further study has been performed. The DC06 MC sample of inclusive $\rm b\overline{b}$ (long life background) used in this note gives an uncertainty for the B/S ratio of the order of 20%. We have performed toy MC studies where the total B/S was set to zero and to 3 times its estimated value. This study provides some extreme boundaries for the effect of the level of background to the $\sin 2\beta$ error. Results for the $\sin 2\beta$ error are summarized in

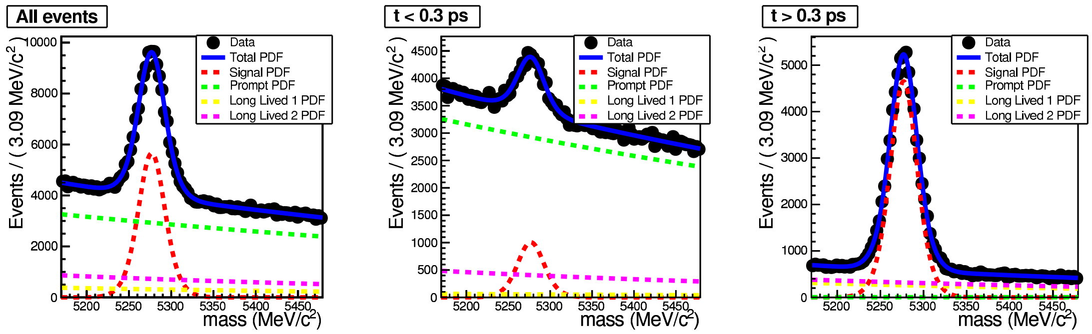


Figure 12: Generated and fitted distribution for $J/\psi K_S^0$ mass according to the lifetime unbiased model. Distributions for small and large proper times are also shown.

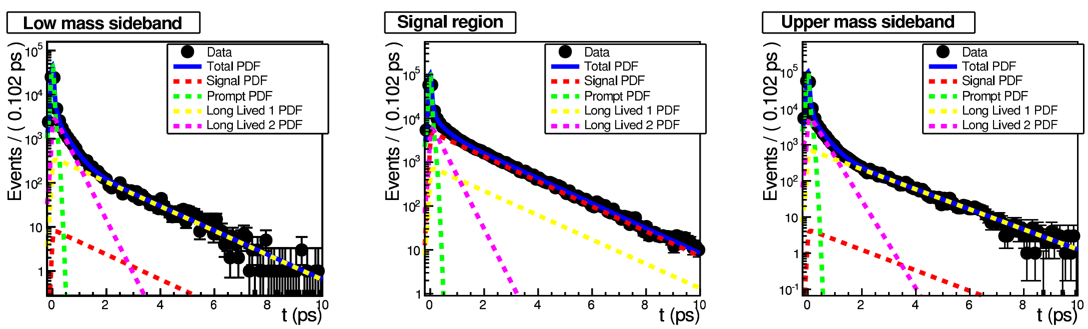


Figure 13: Generated and fitted distribution for $J/\psi K_S^0$ proper time according to the lifetime unbiased model. Distribution for high mass sideband is also shown.

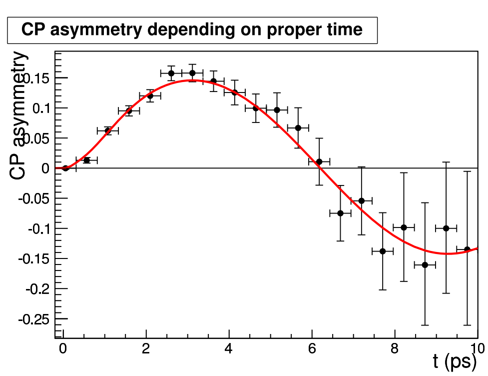


Figure 14: Generated and fitted distribution for $J/\psi K_S^0$ proper time asymmetry according to the lifetime unbiased model.

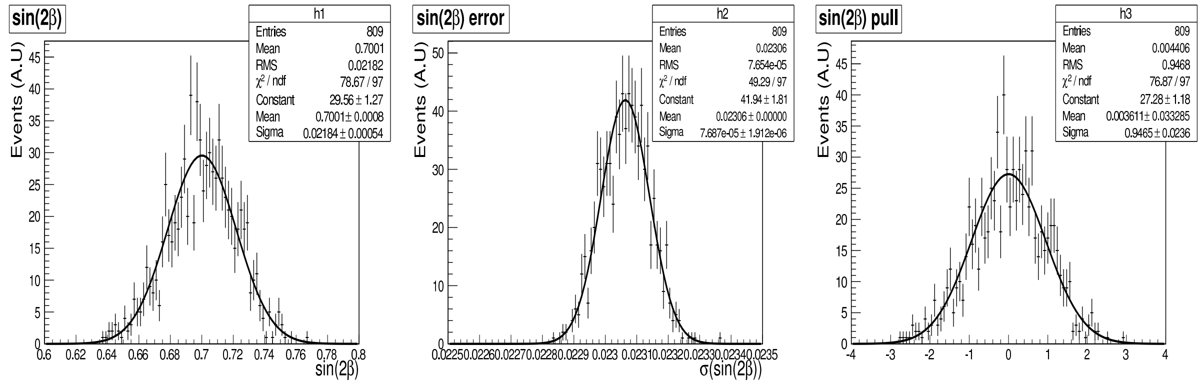

(a) (b) (c)

Figure 15: (a) Distribution for the fitted value of $\sin 2\beta$ from toy samples according to the lifetime unbiased model; (b) Distribution of $\sin 2\beta$ error; (c) Distribution of $\sin 2\beta$ pull.

| **Fixed parameters** | | | |
|---|---|---|---|
| **Parameter** | **Initial value** | | |
| $\Delta m_{\rm d}$ ( $\rm ps^{-1}$ ) | 0.507 | | |
| signal time resolution $\sigma_{t1}^{\rm sig}$ (ps) | 0.037 | | |
| signal time resolution $\sigma_{t2}^{\rm sig}$ (ps) | 0.090 | | |
| fraction of Gauss1 in time res. $f_{\rm time}^{\rm sig}$ | 0.80 | | |
| $\omega_{\rm tag}$ | 0.359 | | |
| **Free parameters** | | | |
| **Parameter** | **Initial value** | **Fitted value** | **Glob. corr.** |
| N events signal | 93800 | $93748 \pm 1447$ | 0.99 |
| N events Prompt | 30000 | $31474 \pm 751$ | 0.94 |
| N events LLived 1 | 23587 | $23511 \pm 712$ | 0.88 |
| N events LLived 2 | 79413 | $78414 \pm 1175$ | 0.88 |
| $M_{\rm B}$ ( MeV/$c^2$) | 5277.0 | 5277.0 $\pm$0.1 | 0.13 |
| $\sigma_{\rm mass1}^{\rm sig}$ ( MeV/$c^2$) | 13.6 | $13.3 \pm 0.2$ | 0.82 |
| $\sigma_{\rm mass2}^{\rm sig}$ ( MeV/$c^2$) | 22.2 | 21.5$\pm$0.2 | 0.70 |
| ${\rm frac}_{\rm mass1}^{\rm sig}$ | 0.56 | 0.52 $\pm$0.02 | 0.89 |
| mass slope Prompt ( MeV/$c^2)^{-1}$ | $-0.8 \cdot 10^{-3}$ | $(-0.83 \pm 0.09) \cdot 10^{-3}$ | 0.35 |
| mass slope LLived ( MeV/$c^2)^{-1}$ | $-1.4 \cdot 10^{-3}$ | $(-1.36 \pm 0.04) \cdot 10^{-3}$ | 0.43 |
| background $\tau^{\rm LL1}$ (ps) | 1.570 | $1.572 \pm 0.019$ | 0.65 |
| background $\tau^{\rm LL2}$ (ps) | 0.453 | $0.455 \pm 0.004$ | 0.68 |
| $\sigma_{\rm gauss}^{\rm Pr}$ (ps) | 0.256 | $0.364 \pm 0.037$ | 0.85 |
| $\sigma_{\rm landau}^{\rm Pr}$ (ps) | $2.24 \cdot 10^{-2}$ | $(2.24 \pm 0.02) \cdot 10^{-2}$ | 0.79 |
| ${\rm mean}_{\rm landau}^{\rm Pr}$ (ps) | $6.09 \cdot 10^{-2}$ | $(6.09 \pm 0.04) \cdot 10^{-2}$ | 0.80 |
| $\tau^{\rm sig}$ (ps) | 1.536 | 1.532$\pm$0.006 | 0.29 |
| $\sin 2\beta$ | 0.700 | 0.713$\pm$0.020 | 0.06 |

Table 15: Input parameters for the $\sin 2\beta$ fit and results of a single toy, according to the lifetime biased model.

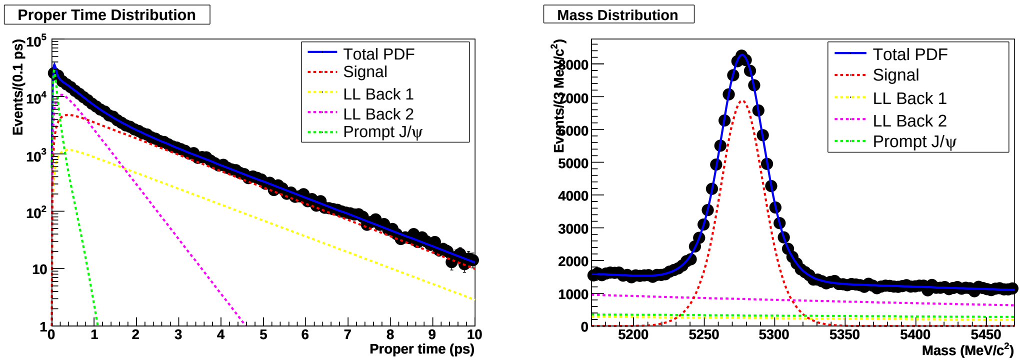


(a) (b)

Figure 16: Generated and fitted distribution for $J/\psi K^0_S$ (a) proper time and (b) mass according to the lifetime biased model.

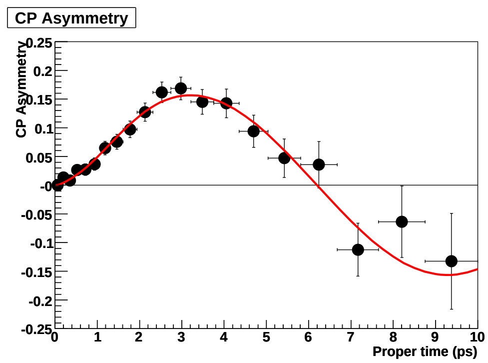


Figure 17: Generated and Fitted distribution for proper time asymmetry according to the lifetime biased model.

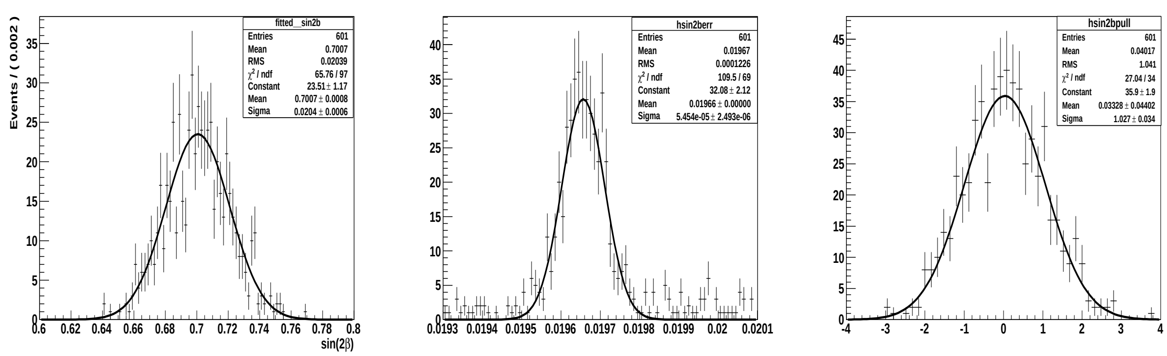


(a) (b) (c)

Figure 18: (a) Distribution for the fitted value of $\sin 2\beta$ from toy samples according to the lifetime biased model; (b) Distribution of $\sin 2\beta$ error; (c) Distribution of $\sin 2\beta$ pull.

| Lifetime Unbiased | | Lifetime Biased | |
| --- | --- | --- | --- |
| B/S | $\sin 2\beta$ error | B/S | $\sin 2\beta$ error |
| 0 | 0.021 | 0 | 0.018 |
| 0.42 | 0.023 | 0.36 | 0.020 |
| $3 \times 0.42$ | 0.025 | $3 \times 0.36$ | 0.022 |

Table 16: Dependence of $\sin 2\beta$ and its error on the level of B/S for the long life background. The errors on these values are of the order of $10^{-4}$ or less.

Table 16 for the three hypotheses: B/S = 0; expected B/S; 3×B/S. No biases are seen for the $\sin 2\beta$ mean value.

## 5.3 Some systematic studies for $\sin 2\beta$

To estimate the level of systematic uncertainties in the $\sin 2\beta$ measurement for 2fb$^{-1}$ data, some studies have been performed and are described here, both for the lifetime unbiased and biased selections. In all cases, the systematic errors found come from toy MC studies with many hundreds of samples. We address possible systematic effects due to uncertainties on the mistag rate and lifetime acceptance correction.

### 5.3.1 Uncertainty on mistag rate, $\omega$

As we have shown in Section 4, the combined values obtained for $\omega$ in $B^0 \to J/\psi K^0_S$ and $B^0 \to J/\psi K^{*0}$ channels agree well, their difference being $\omega_{KS} - \omega_{K^*} = (0.55 \pm 0.39) \times 10^{-2}$. The relative statistical error for $\omega$ from $B^0 \to J/\psi K^{*0}$ for 2 fb$^{-1}$ is estimated to be 0.3%, with a negligible systematic error due to the background. Thus a relative uncertainty on the value for $\omega$ is expected to be below 1%.

We have performed toy MC studies by introducing a bias on the value of $\omega$. Samples were generated using the central value $\omega = 0.359$ while were fitted assuming the $\pm 1\%$ variation, $\omega_{\rm lower} = 0.355$ and $\omega_{\rm higher} = 0.363$. The study was performed for both lifetime unbiased and biased selections. The results are displayed in Table 17. We see that $\sin 2\beta$ is biased by almost $1\sigma$ (statistical) due to an 1% relative uncertainty on the mistag.

Indeed we can estimate the resulting bias on $\sin 2\beta$ due to a bias in the mistag, $\omega' = \omega + \Delta\omega$:

$$\text{bias}(\sin 2\beta) = 1 - \frac{1 - 2\omega'}{1 - 2\omega} = \frac{2\Delta\omega}{1 - 2\omega} \; . \tag{9}$$

For $\omega = 0.36$ with a relative bias of 1%, a 2.6% bias on $\sin 2\beta$ results from the expression above, which agrees with the $1\sigma$ statistical error (for 2 fb$^{-1}$) we found. In Fig. 19 we show the resulting bias on $\sin 2\beta$ for relative variations of 1%, 0.5% and 0.1% on the mistag rate.

Differences between flavour tagging performance for b and $\overline{\rm b}$ mesons are not addressed here. They can arise from production or detection asymmetries. Detection asymmetries are a consequence, for example, of the different interaction cross section for positive and negative kaons and possible charge asymmetries in the tracking. The observed difference in the mistag rate for b and $\overline{\rm b}$ in the Monte Carlo data is not significant with the available

| Model | $\omega$ | $\sin 2\beta$ | $\sin 2\beta$ error | $\sin 2\beta$ pull |
|---|---|---|---|---|
| Lifetime Unbiased | 0.355 | $0.680 \pm 0.001$ | 0.022 | $-0.90 \pm 0.04$ |
| | 0.363 | $0.721 \pm 0.001$ | 0.024 | $0.87 \pm 0.04$ |
| Lifetime Biased | 0.355 | $0.679 \pm 0.002$ | 0.019 | $-1.18 \pm 0.11$ |
| | 0.363 | $0.720 \pm 0.001$ | 0.020 | $1.08 \pm 0.06$ |

Table 17: Results for $\sin 2\beta$ mean, error and pull by introducing a 1% relative variation on the expected value of the mistag rate. Assuming 2 $\mathrm{fb}^{-1}$ of data.

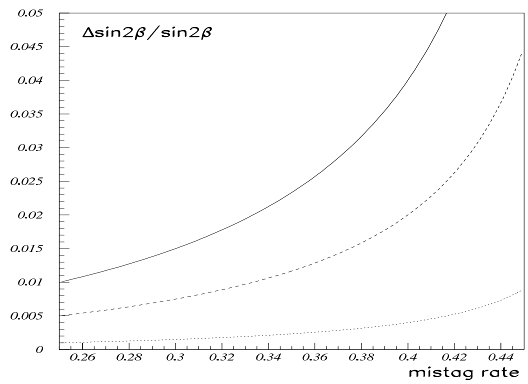


Figure 19: Bias on $\sin 2\beta$ due to a bias on the mistag. The three curves are for relative variations of 1%, 0.5% and 0.1% on the mistag rate, respectively.

sample sizes [12], at this level they would be below the statistical error on the mistag rate for 2 $\mathrm{fb}^{-1}$. However, the mistag rates will be measured separately on b and $\overline{\mathrm{b}}$ events in the data in the flavour-specific control channels, and the two different values can be explicitly introduced in the CP fit.

### 5.3.2 Uncertainty due to the propertime acceptance correction

- Lifetime unbiased selection

  As the name implies, this selection is based on a set of cuts which do not introduce any significative bias in the propertime distribution.We have performed tests where a weak linear dependence of the acceptance on the propertime was introduced in the toy generated samples, while the fitting function included (as in our standard lifetime unbiased study) any acceptance correction. The included acceptance was a linear function acc $= -0.001t + 0.07$ (ps) and the result from 893 toy MC samples has shown no effect on the mean value of the distribution for $\sin 2\beta$ ($\sin 2\beta = 0.7003 \pm 0.0008$), with pull $0.01 \pm 0.03$. Nevertheless, the measured lifetime is affected, with a pull of $-5.13 \pm 0.03$.

- Lifetime biased selection

  We have varied the slope of the acceptance function for generating the toy MC samples while fitting with the function given in Fig. 5. The slope has been varied to $a = -4.5$ $\mathrm{ps}^{-1}$ and $a = -9.0$ $\mathrm{ps}^{-1}$. In both cases, we found no significative variation in the $\sin 2\beta$ value or error. Results are presented in Table 18.

| $a$ ($ps^{-1}$) | $\sin 2\beta$ | $\sin 2\beta$ error | $\sin 2\beta$ pull |
|---|---|---|---|
| $-4.5$ | $0.701 \pm 0.001$ | 0.0194 | $0.05 \pm 0.06$ |
| $-9.0$ | $0.700 \pm 0.002$ | 0.0200 | $0.05 \pm 0.06$ |

Table 18: Results for $\sin 2\beta$ mean, error and pull by changing the slope of the acceptance function for the generated toy samples for the biased lifetime model. Assuming 2 $fb^{-1}$ of data.

# 6 Summary and conclusions

In this note, we have presented an update of the $B^0 \to J/\psi(\mu\mu)K^0_S$ analysis. The channel $B^0 \to J/\psi(\mu\mu)K^0_S$ is the gold-plated mode for the extraction of $\sin(2\beta)$.

Using DC06 samples, for a lifetime unbiased selection we have estimated an annual yield of 193k $B^0 \to J/\psi(\mu\mu)K^0_S$ events after L0 trigger, with a background to signal ratio B/S=0.42 for $b\overline{b}$ inclusive events, and B/S=3.01 for prompt $J/\psi$. For a lifetime biased selection, the yield goes to 208k and B/S goes down to 0.36 and 0.27 for $b\overline{b}$ inclusive and prompt $J/\psi$, respectively.

To assess the sensitivity on $\sin(2\beta)$ we have generated toy Monte Carlo events using the expected yields after triggers and tagging for signal and background, lifetime information, and mistag rate as inputs. We estimate that after 2 $fb^{-1}$ of data taking, the statistical LHCb sensitivity to $\sin(2\beta)$ is 0.023 for a lifetime unbiased selection, and can be improved down to 0.020 with a lifetime biased selection. We have performed some systematic studies by including variations on the mistag rate and on the acceptance function. The latter did not shown any significant impact. The mistag rate, as expected, gives a significant effect, a 1% relative mismatch between true and measured mistag rate introduce a systematic error of the order of $1\sigma$ for $2fb^{-1}$ of data.

# Acknowlegments

This work has been partially supported by ALFA-EC funds in the framework of HELEN Project, and by the Brazilian funding agencies CNPq, FAPERJ, RENAFAE and FINEP.

# A Composition of the inclusive $b\overline{b}$ sample.

A closer look at the 24 events that survive the unbiased selection, shows that most of them are a combination of a true $J/\psi \to \mu^+\mu^-$ originating from a B meson, and a true $K^0_S$ coming from elsewhere. In LHCb there is a standard way of categorizing the background [9] and the ones that are present in this analysis are:

- Reflection - This background is caused by the misidentification of a final state particle. In this case, a kaon is misidentified as a pion.
- Low mass background - A fragment of a decay occurring in the event is incorrectly identified as a signal decay. One example here would be a true $J/\psi$ from a $B^+$.
- Ghost - At least one of the final state particles does not have an associated MC Particle.

- From PV - The candidate particle has at least one final state daughter which comes directly from the primary vertex or a short lived resonance, and the event is not a pileup.
- All from same PV - The candidate particle's final state daughters all come from the same PV, or from short lived resonances from the same PV.
- From different PV - Pileup - Any reconstructed decay in which the final-state particles come from more than one primary vertex.
- $b\overline{b}$ - Any background which does not fit into any of the previous categories, but in which, at least one of the final state particles has a mother with bottom content.

Table 19 shows the details of the composition of these events according to this classification, and in case they are from $b\overline{b}$ , the detailed decay tree is shown. In Table 20 the equivalent for the 21 events surviving the biased selection is shown.

| classification | Nr. Events |
|---|---|
| Reflection | 1 LL |
| Low mass background | 1 LL, 3 DD |
| Ghost | 1 LL, 1 DD |
| From PV | 1 LL, 2 DD |
| From different PV | 1 DD |
| $b\overline{b}$ | |
| true $J/\psi \rightarrow \mu^+\mu^-$ from B<br>true $K^0_S \rightarrow \pi^+\pi^-$ from PV | 7 DD |
| true $\mu$ from B<br>true $K^0_S \rightarrow \pi^+\pi^-$ from PV | 1 LL ,1 DD |
| true $J/\psi \rightarrow \mu^+\mu^-$ from B<br>true $\pi$ from $\omega(782)$ from B | 1 LL |
| true $J/\psi \rightarrow \mu^+\mu^-$ from $\Lambda_b$<br>true $K^0_S \rightarrow \pi^+\pi^-$ from PV | 1 DD |
| true $\mu$ from $\Lambda_b$<br>true $K^0_S \rightarrow \pi^+\pi^-$ from PV | 1 DD |
| true $\mu$ from $\Lambda_b$<br>true $K^0_S \rightarrow \pi^+\pi^-$ from PV | 1 DD |

Table 19: Composition of background events passing the unbiased $B^0 \rightarrow J/\psi(\mu\mu)K^0_S$ selection in an enlarged mass window of an inclusive $b\overline{b}$ sample.

| classification | Nr. Events |
|---|---|
| Low mass background | 3 LL, 4 DD |
| From different PV | 3 DD |
| true $J/\psi \rightarrow \mu^+\mu^-$ from B | 6 LL, 5 DD |
| true $K^0_S \rightarrow \pi^+\pi^-$ from PV | |

Table 20: Composition of background events passing the biased $B^0 \rightarrow J/\psi(\mu\mu)K^0_S$ selection in an enlarged mass window of an inclusive $b\overline{b}$ sample.

# References


[1] I.I. Bigi and A.I.Sanda, *CP Violation*, Cambridge Univ.Press (2000).

[2] P. Ball *et al.*, hep-ph/0003238 (CERN-TH/2000-101).

[3] B. Albert *et al.* (BaBar Collaboration), Phys.Rev.Lett. **99**, 171803 (2007).

[4] K.-F. Chen *el et.* (Belle Collaboration), Phys.Rev.Lett.**98**, 031802 (2007).

[5] Heavy Flavor Averaging Group, Unitarity Triangle Working Group, Latest Update, http://www.slac.stanford.edu/xorg/hfag/triangle/latest/#sin2b.

[6] http://www.thep.lu.se/ tobjorn/Pythia.html.

[7] http://geant4.web.cern.ch/geant4.

[8] R. Antunes Nobrega *et al.*, "Reoptimized LHCb Detector, Design and Performance", CERN-LHCC/2003-030.

[9] V.V. Gligorov, "Reconstruction of Channel $B^0 \rightarrow D^+\pi^-$ and Background Classification at LHCb" LHCb-2007-044, V.V. Gligorov LHCb Note 2007-052.

[10] C. Amsler *et al.*(Particle Data Group), Physics Letters B **667**, 1 (2008).

[11] M. Calvi, O. Leroy, M. Musy, "Flavour Tagging Algorithms and Performances in LHCb", CERN-LHCb-2007-058.

[12] M. Calvi, G. Lanfranchi, O. Leroy, M. Musy, S. Poss and S. Vecchi, "Calibration of Flavour Tagging with $B^+ \rightarrow J/\psi K^+$ and $B^0 \rightarrow J/\psi K^{*0}$ control channels at LHCb", CERN-LHCb-2009-020.

[13] M. Calvi, B. Khanji, G. Lanfranchi, O. Leroy and S. Poss, "Lifetime Unbiased Selection of $B^0_s \rightarrow J/\psi\phi$ and related control channels: $B^0 \rightarrow J/\psi K^*$ and $B^+ \rightarrow J/\psi\ K^+$", CERN-LHCb-2009-025.

[14] W. Verkerke and D. Kirkby, http://roofit.sourceforge.net.